Synthesis and Integration of Multifunctional Oxide Materials

April 22, 2009
NCC AVS Thin Film User Group

Jane P. Chang
Ryan Martin, Lin Sha, Carey Tanner, Trinh Van
Department of Chemical and Biomolecular Engineering
University of California, Los Angeles, CA 90095

Outline

- Motivation
  - Multifunctional Oxide Materials
  - Versatile applications
- Patterning of complex metal oxides
  - Challenges
  - Criteria in selecting plasma chemistries
  - Simple metal oxides (ZrO_2 and HfO_2)
  - Complex HfO_2 based dielectrics ($HfAl_xO_y$, $HfSi_xO_yN_z$)
- Reaction mechanisms in patterning metal oxides
  - Modeling competition between etch and deposition
- Conclusion
- Acknowledgement

ALD, an enabler for nano-patterning

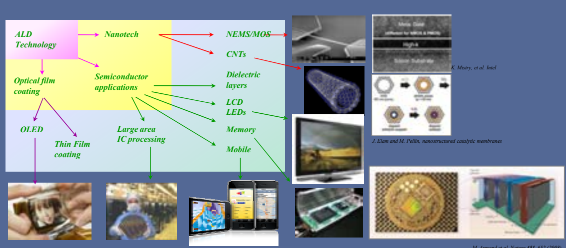

- Conformal and well controlled synthesis of metals, semiconductors, and complex oxides
- Integration with subtractive or additive processes to form nano-patterns

Multifunctional Metal Oxides

Dielectric	κ	E_{BD} (MV/cm)	E_g (eV)
SiO_2	3.9	12-15	8-9
SiO_xN_y	~4	15-16	6
Si_3N_4	7-9	10-11	5
TiO_2	80-120	0.5	4
Ta_2O_5	20-25	3-5	3-4
ZrO_2	15-24	15-20	5-7
HfO_2	15-24	15-20	5-7
Al_2O_3	9-12	10	8
Y_2O_3	12-15	4-5	6
Er_2O_3	10-14	8-17	6

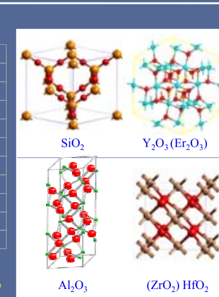

- ZrO_2/HfO_2 have high κ, large E_{BD}, and wide band gap
- Y_2O_3/Er_2O_3 have medium κ, E_{BD}, and wide band gap

Chang, J. P., Book Chapter on "High-K Gate Dielectric Deposition Technology Survey" in *High-K Gate Dielectric Materials for VLSI MOSFET*, Springer-Verlag (2005).

Challenges in High-k Etch

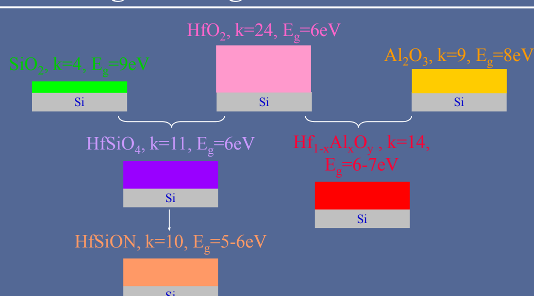

- Si, Al, and N incorporations have been shown to improve the dielectric properties, the crystallization temperature, and band alignment with respect to silicon

Outline

- Motivation
  - Multifunctional Oxide Materials
  - Versatile applications
- Patterning of complex metal oxides
  - Challenges
  - Criteria in selecting plasma chemistries
  - Simple metal oxides (ZrO_2 and HfO_2)
  - Complex HfO_2 based dielectrics ($HfAl_xO_y$, $HfSi_xO_yN_z$)
- Reaction mechanisms in patterning metal oxides
  - Modeling competition between etch and deposition
- Conclusion
- Acknowledgement

Criteria in Plasma Selection

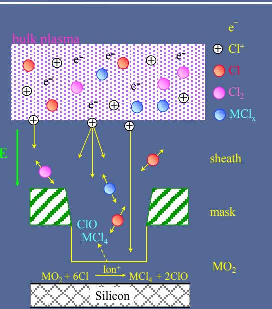

- Etching of high-k dielectrics
  - Metal oxides
  - Doped metal oxides
  - Alloyed metal oxides
- Important criteria
  - Plasma chemistry
  - Plasma density, ion energy
  - Dominant etch species
  - Metal oxygen bond strength
  - Nature of etching products
  - Heat of reaction
  - Etch product volatility

- Cl_2 and BCl_3 plasma are viable for patterning high-k dielectrics

Chang Lab UCLA

Reaction Pathways

Potential Reactions in Cl_2

Chemical Reactions	ΔH (kJ/mol)
$Cl_2 \xrightarrow{k_1} 2Cl$	243
$Cl + O \xrightarrow{k_2} ClO$	-268
$Al_2O_3 \xrightarrow{k_3} 2Al + 3O$	3084
$Al_2O_3 + 2Cl \xrightarrow{k_4} 2AlCl + 3O$	2085
$Al_2O_3 + 4Cl \xrightarrow{k_5} 2AlCl_2 + 3O$	1276
$Al_2O_3 + 6Cl \xrightarrow{k_6} 2AlCl_3 + 3O$	529
$Al_2O_2 + 5Cl \xrightarrow{k_7} 2AlCl + 3ClO$	1279
$Al_2O_3 + 7Cl \xrightarrow{k_8} 2AlCl_2 + 3ClO$	470
$Al_2O_3 + 9Cl \xrightarrow{k_9} 2AlCl_3 + 3ClO$	-277
$HfO_2 \xrightarrow{k_{10}} Hf + 2O$	2261
$HfO_2 + 4Cl \xrightarrow{k_{11}} HfCl_4 + 2O$	271
$HfO_2 + 6Cl \xrightarrow{k_{12}} HfCl_4 + 2ClO$	-264

Potential Reactions in BCl_3

Chemical Reactions	ΔH (kJ/mol)
$BCl_3 + \frac{1}{2}O_2 \longrightarrow \frac{1}{3}(BOCl)_3 + Cl_2$	-141
$Al_2O_3 + 3BCl_{3(g)} \longrightarrow 2AlCl_{3(g)} + (BClO)_{3(g)}$	84
$Al_2O_3 + 6BCl_{3(g)} \longrightarrow 2AlCl_{3(g)} + 3B_2OCl_{4(g)}$	286
$Al_2O_3 + \frac{9}{2}BCl_{3(g)} \longrightarrow 2AlCl_{3(g)} + \frac{3}{2}B_3O_2Cl_{5(g)}$	250
$HfO_2 + 2BCl_{3(g)} \longrightarrow HfCl_{4(g)} + \frac{2}{3}(BClO)_{3(g)}$	-58
$HfO_2 + 4BCl_{3(g)} \longrightarrow HfCl_{4(g)} + 2B_2OCl_{4(g)}$	79
$HfO_2 + 3BCl_{3(g)} \longrightarrow HfCl_{4(g)} + B_3O_2Cl_{5(g)}$	53

Species Volatility

Metal Halides	Sublimation Pt. (°C)
AlF_3	1276
$AlCl_3$	180
$AlBr_3$	255
AlI_3	382
HfF_4	970
$HfCl_4$	317
$HfBr_4$	323
HfI_4	394

Species Volatility

Metal Halides	Sublimation Pt. (°C)
$AlCl_3$	180
$HfCl_4$	317

Bond Strength

Bond	Bond Strength (eV)
Al-O	5.31
Al-Cl	5.31
Hf-O	8.32
Hf-Cl	5.16

- MCl_x, ClO, and $(BOCl)_3$ formation drives the etching reactions

Chang Lab UCLA

Plasma Diagnostics

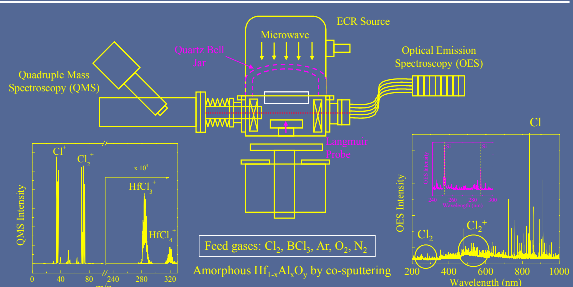

Feed gases: Cl_2, BCl_3, Ar, O_2, N_2

Amorphous $Hf_{1-x}Al_xO_y$ by co-sputtering

- Quantify gas phase and surface reactions by LP, OES, QMS and XPS
- $ER_{M,M_xO} = f\left(J_{etch}, J_{dep}, F_{M_xO_y}, \theta, J_n/J_+, \sqrt{E_{ion}}\right)$

Chang Lab UCLA

BCl_3/Cl_2 Plasma Characterization

QMS Measurement | Langmuir probe Measurement

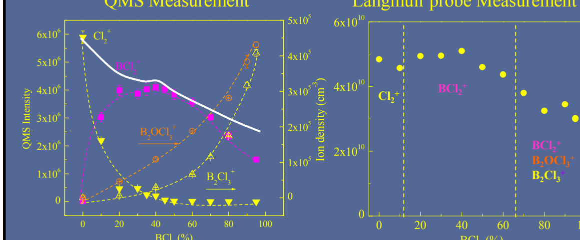

- 5 mTorr, 300 W, -70 V; Ar flow rate was fixed at 5%
- BCl_2^+ is the dominant ionic species
- Ion density was maximized at 40% of BCl_3 and reduced at higher BCl_3 flow rate

Chang Lab UCLA

Outline

- Motivation
  - Multifunctional Oxide Materials
  - Versatile applications
- Patterning of complex metal oxides
  - Challenges
  - Criteria in selecting plasma chemistries
  - Simple metal oxides (ZrO_2 and HfO_2)
  - Complex HfO_2 based dielectrics ($HfAl_xO_y$, $HfSi_xO_yN_z$)
- Reaction mechanisms in patterning metal oxides
  - Modeling competition between etch and deposition
- Conclusion
- Acknowledgement

Chang Lab UCLA

Effect of Ion Type/Energy on ER

Cl_2 | 3 mTorr, 500 W | BCl_3

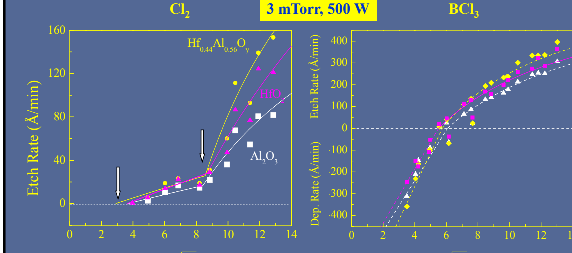

- Etching rate increases scales with the square root of ion energy and BCl_3 addition
- Etching threshold energy depends on the M-O bond strength

Chang Lab UCLA

Effect of Ion Type/Energy on ER

Cl_2 | 3 mTorr, 500 W | BCl_3

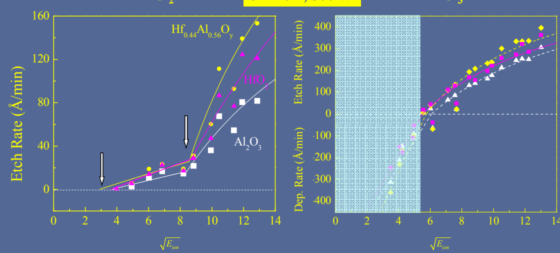

- Etching rate increases scales with the square root of ion energy and BCl_3 addition
- Etching threshold energy depends on the M-O bond strength

Effect of Ion Type/Energy on EP

Cl_2 | $Hf_{0.44}Al_{0.56}O_y$; 3 mTorr, 500 W | BCl_3

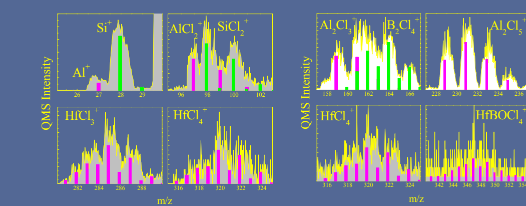

- Al, $AlCl_2$, Al_2Cl_3, and Al_2Cl_5 identified as the primary Al-containing etch products in BCl_3
- Hafnium removed as $HfCl_3$, $HfCl_4$, and $HfBOCl_4$ in BCl_3 plasma
- Etch product formation increases with E_i

Effect of Ion Type/Energy on EP

Cl_2 | $Hf_{0.44}Al_{0.56}O_y$; 3 mTorr, 500 W | BCl_3

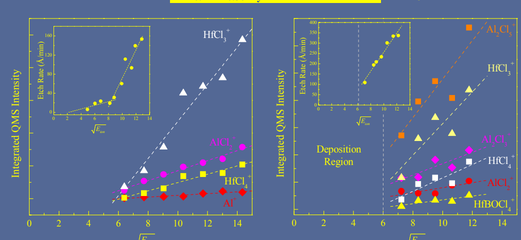

- Al, $AlCl_2$, Al_2Cl_3, and Al_2Cl_5 identified as the primary Al-containing etch products in BCl_3
- Hafnium removed as $HfCl_3$, $HfCl_4$, and $HfBOCl_4$ in BCl_3 plasma
- Etch product formation increases with E_i

Surface Composition

Cl_2 | $Hf_{0.44}Al_{0.56}O_y$; 3 mTorr, 500 W | BCl_3

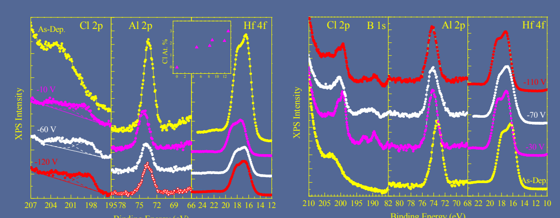

- Boron (~3-5 at. %) and chlorine (~1-2 at. %) observed upon etched film surfaces
- Surface composition (Hf, Al, O) relatively constant after etching
- Amount of B and Cl increase with decreasing E_{ion}; deposition dominates at lower E_{ion}

Cl_2/BCl_3 Plasmas – Effects on ER

3mTorr, 500W | E_{ion} ~80eV | 5mTorr, 300W

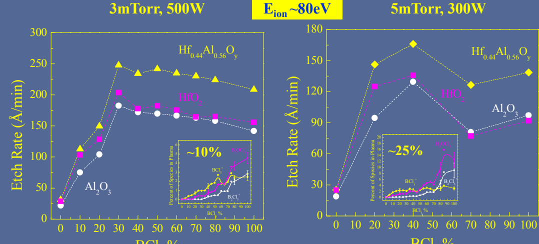

- Etch rate increases possibly due to increasing amount of high mass species

$$E.R.(Cl^+, Cl_2^+) \le E.R.(BCl_2^+) \le E.R.(BCl_x^+, B_xO_yCl_z^+)$$

Etching Mechanism Analysis

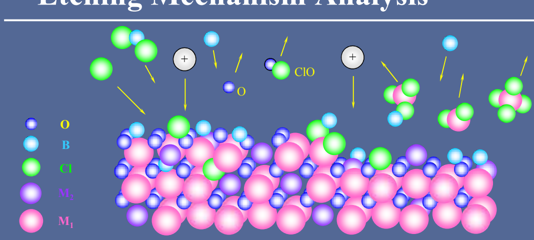

- Breaking M-O bond is the critical step
  - — Chemically enhanced process → ClO, $(BOCl)_3$
- Cl radicals react with M to form volatile MCl_x
- Complexity of surface reactions (similar trends for $HfSi_xO_yN_z$)
  - — Simplifications necessary for modeling

Etch Selectivity to Silicon

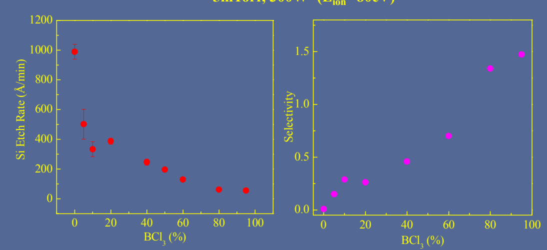

- High selectivity is required for patterning advanced gate stack

A Two-Step Etching Process

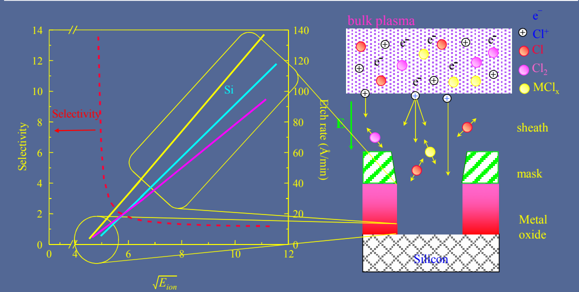

- Higher threshold energy was obtained for etching Si in BCl_3 plasma
- Low ion energy is preferred towards the end of the etching

Outline

- Motivation
  - Multifunctional Oxide Materials
  - Versatile applications
- Patterning of complex metal oxides
  - Challenges
  - Criteria in selecting plasma chemistries
  - Simple metal oxides (ZrO_2 and HfO_2)
  - Complex HfO_2 based dielectrics ($HfAl_xO_y$, $HfSi_xO_yN_z$)
- Reaction mechanisms in patterning metal oxides
  - Modeling competition between etch and deposition
- Conclusion
- Acknowledgement

Plasma Etch Modeling: Review

Steinbrüchel (1989) — sputtering by ions

$$Y(E) = C_{pt}S_n(E/E_{pt})f(E_{th}/E)$$
$$S_n(E/E_{pt}) \propto E^{1/2}$$
$$f_M(E_{th}/E) = 1-(E_{th}/E)^{1/2}$$
$$R \approx A\left(E^{1/2}-E_{th}^{1/2}\right)$$

Gottscho/Sawin (82/93) — etching by neutrals/ions

$$R = k\Theta E_i J_i$$
$$R = vS_0(1-\Theta)J_n$$
$$\Theta = \frac{1}{1+kE_iJ_i/(vS_0J_n)}$$
$$R = \frac{kE_iJ_i}{1+kE_iJ_i/(vS_0J_n)}$$

Hershikowitz (1996) — etching and deposition

$$(ER)_{i\alpha} = K_{e\alpha}\theta_{e\alpha}J_iE_i$$
$$(DR)_{i\alpha} = K_{d\alpha}\theta_{d\alpha}J_iE_i$$
$$\theta_s+\theta_p = 1$$
$$\theta_s = \theta_{es}+\theta_{ds}+\theta_1$$
$$\theta_p = \theta_{ep}+\theta_{dp}+\theta_2$$
$$R_t = \frac{K_{es}J_iE_i\left[1-C_{sp}\left(\frac{J_d}{J_e}\right)^2\right]}{1+A_s\frac{J_iE_i}{J_e}+B_s\frac{J_d}{J_e}\left[1+\frac{K_{ds}}{K_{ep}}\left(1+A_p\frac{J_iE_i}{J_e}+B_p\frac{J_d}{J_e}\right)\right]}$$

Pearton (2006) — spontaneous /ion-assisted desorption

$$ER = (J_+Y_{sat}+k_{sat})\theta_n/N_t$$
$$Y_{sat} = A_{sat}\left(\sqrt{E_+}-\sqrt{E_{th}}\right)$$
$$\theta_n = \frac{1}{1+\beta(J_+Y_{sat}+k_{sat})/J_nS_n}$$
$$k_{sat} = J_+B_{sat}\left(\sqrt{E_+}-\sqrt{E_{dis}}\right)$$
$$R = \frac{J_+\left[A_{sat}\left(\sqrt{E_+}-\sqrt{E_{th}}\right)+B_{sat}\left(\sqrt{E_+}-\sqrt{E_{dis}}\right)\right]/N_t}{1+J_+\left[\beta_{mv}A_{sat}\left(\sqrt{E_+}-\sqrt{E_{th}}\right)+\beta_v B_{sat}\left(\sqrt{E_+}-\sqrt{E_{dis}}\right)\right]/J_nS_n}$$

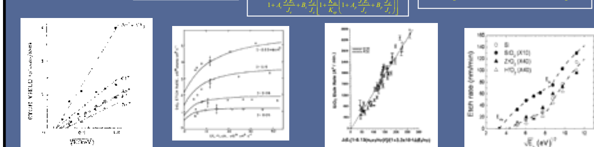

- Challenges: flux/energy dependence and etch/deposition competition

Barker, Mayer, et al. JVSTB 1(1) (1983), Steinbrüchel APL 55(17) (1989), Gottscho, Jurgensen, et al., JVSTB 10(5) 1992, Ding, Hershkowitz, APL 68(12) (1996), Stafford, Pearton, et al., JAP 100(6) (2006)

Modeling Formulation

$$E_{ion} > E_{th,s} \quad (E_{th,s} > E_{th,p})$$

Etch rate of metal oxide

$$(ER)_s = J_iA_s\left(E_{ion}^{1/2}-E_{th,s}^{1/2}\right)\theta_{es}+J_iB_s\left(E_{ion}^{1/2}-E_{tr,s}^{1/2}\right)\theta_{es} = J_ev_{es}S_{es}\theta_1$$

Deposition rate on metal oxide

$$(DR)_s = D_s\theta_{ds} = J_dv_{ds}S_{ds}\theta_1$$

Etch rate of polymer

$$(ER)_p = J_iC_p\left(E_{ion}^{1/2}-E_{th,p}^{1/2}\right)\theta_{ep} = J_ev_{ep}S_{ep}\theta_2$$

Deposition rate of polymer

$$(DR)_p = D_p\theta_{dp} = J_dv_{dp}S_{dp}\theta_2$$

Site balance

$$\theta_s+\theta_p = 1 \Rightarrow \theta_1+\theta_{es}+\theta_{ds}+\theta_2+\theta_{ep}+\theta_{dp} = 1$$

Total reaction rate:

$$R_t = (ER)_s \boxed{-(DR)_s+(ER)_p} -(DR)_p = (ER)_s-(DR)_p = J_iA_s\left(E_{ion}^{1/2}-E_{th,s}^{1/2}\right)\theta_{es}+J_iB_s\left(E_{oni}^{1/2}-E_{tr,s}^{1/2}\right)\theta_{es}-D_p\theta_{dp}$$

Summary of Rate Model Parameters

Parameter	Definition	Units
J_i	Positive ion flux	$\#/Å^2 s$
J_e	Etching Species flux	
J_d	Depositing species flux	
E_{ion}	Positive ion energy	eV
$E_{th,s}$	Substrate etching threshold energy	
$E_{tr,s}$	Substrate etching transition energy	
$E_{th,p}$	Polymerching threshold energy	
v_{es}	Volume of substrate removed per etching species	$Å^3/\#$
v_{ds}	Volume of polymer grown on substrate per depositing species	
v_{ep}	Volume of polymer removed per etching species	
v_{dp}	Volume of polymer grown on polymer per depositing species	
S_{es}	Reactive sticking probability of etching species on substrate	*unitless*
S_{ds}	Reactive sticking probability of depositing species on substrate	
S_{ep}	Reactive sticking probability of etching species on polymer	
S_{dp}	Reactive sticking probability of depositing species on polymer	
A_s	Volume of substrate removed per unit bombardment energy due to ion mixing-induced desorption	$Å^3/eV^{1/2}$
B_s	Volume of substrate removed per unit bombardment energy due to ion-enhanced chemical etching	
C_p	Volume of polymer removed per unit bombardment energy due to ion-enhanced chemical etching	
D_s	Depositiong rate of polymer on substrate	$Å/s$
D_p	Depositiong rate of polymer on polymer	
$Z_{\alpha\gamma} = v_{\alpha\gamma}S_{\alpha\gamma}$		

R. M. Martin and J. P. Chang, JVST (2009)

Model Development

$$R_t = \frac{J_e^2v_{es}S_{es}v_{ep}S_{ep}-J_d^2v_{ds}S_{ds}v_{dp}S_{dp}}{J_ev_{ep}S_{ep}+\frac{J_d^2v_{ds}S_{ds}v_{dp}S_{dp}}{D_p}+\frac{J_dJ_ev_{ds}S_{ds}v_{ep}S_{ep}}{J_iC_p\left(E_{ion}^{1/2}-E_{th,p}^{1/2}\right)}+J_dv_{ds}S_{ds}+\frac{J_dJ_ev_{ds}S_{ds}v_{ep}S_{ep}}{D_s}+\frac{J_e^2v_{es}S_{es}v_{ep}S_{ep}}{J_i\left[A_s\left(E_{ion}^{1/2}-E_{th,s}^{1/2}\right)+B_s\left(E_{ion}^{1/2}-E_{tr,s}^{1/2}\right)\right]}}$$

$J_d = 0$:

$$R_t = \frac{J_i\left[A_s\left(E_{ion}^{1/2}-E_{th,s}^{1/2}\right)+B_s\left(E_{ion}^{1/2}-E_{tr,s}^{1/2}\right)\right]}{1+J_i\left[A_s\left(E_{ion}^{1/2}-E_{th,s}^{1/2}\right)+B_s\left(E_{ion}^{1/2}-E_{tr,s}^{1/2}\right)\right]/J_ev_{es}S_{es}}$$

$J_e = 0$:

$$R_t = -\frac{J_dv_{dp}S_{dp}}{1+J_dv_{dp}S_{dp}/D_p}$$

In Cl_2 $J_d \approx 0$

$$R_t = \frac{J_i\left[A_s\left(E_{ion}^{1/2}-E_{th,s}^{1/2}\right)+B_s\left(E_{ion}^{1/2}-E_{tr,s}^{1/2}\right)\right]}{1+J_i\left[A_s\left(E_{ion}^{1/2}-E_{th,s}^{1/2}\right)+B_s\left(E_{ion}^{1/2}-E_{tr,s}^{1/2}\right)\right]/J_eZ_{es}}$$

In BCl_3 $J_iA_s\left(E_{ion}^{1/2}-E_{th,s}^{1/2}\right) << J_iB_s\left(E_{ion}^{1/2}-E_{tr,s}^{1/2}\right)$

$$R_t = \frac{J_e^2Z_{es}Z_{ep}-J_d^2Z_{ds}Z_{dp}}{J_eZ_{ep}+\frac{J_d^2Z_{ds}Z_{dp}}{D_p}+\frac{J_dJ_eZ_{ds}Z_{ep}}{J_iC_p\left(E_{ion}^{1/2}-E_{th,p}^{1/2}\right)}+J_dZ_{ds}+\frac{J_dJ_eZ_{ds}Z_{ep}}{D_s}+\frac{J_e^2Z_{es}Z_{ep}}{J_iB_s\left(E_{ion}^{1/2}-E_{tr,s}^{1/2}\right)}}$$

R. M. Martin and J. P. Chang, JVST (2009)

Final Model and Evaluation

$E_{ion} > E_{th,s}$

$$R_t = \frac{J_e^2 Z_{es} Z_{ep} - J_d^2 Z_{ds} Z_{dp}}{\left\{ \begin{array}{l} J_e Z_{ep} + \dfrac{J_d^2 Z_{ds} Z_{dp}}{D_p} + \dfrac{J_d J_e Z_{ds} Z_{ep}}{J_i C_p \left(E_{ion}^{1/2} - E_{th,p}^{1/2}\right)} \\ + J_d Z_{ds} + \dfrac{J_d J_e Z_{ds} Z_{ep}}{D_s} + \dfrac{J_e^2 Z_{es} Z_{ep}}{J_i \left[A_s \left(E_{ion}^{1/2} - E_{th,s}^{1/2}\right) + B_s \left(E_{ion}^{1/2} - E_{tr,s}^{1/2}\right)\right]} \end{array} \right\}}$$

$E_{th,p} < E_{ion} < E_{th,s}$

$$R_t = (E.R.)_{ep} - (D.R.)_{dp} = J_i C_p \left(E_{ion}^{1/2} - E_{th,p}^{1/2}\right) - J_d Z_{dp}$$

$E_{ion} < E_{th,p}$

$$R_t = -(D.R.)_{dp} = -J_d v_{dp} S_{dp} = -J_d Z_{dp}$$

- $-(D.R.)_{dp}$ = 300 Å/min
- J_d = 26 #/Å²s
- S_{dp} of BCl_x ranges 0.001 to 0.1*
- → v_{dp} ~ 19 Å³

* Choi and Veerasingam JVST A **16**(3), 1873 (1998).

Modeling of ER in Cl_2

Cl_2 3 mTorr, 500 W

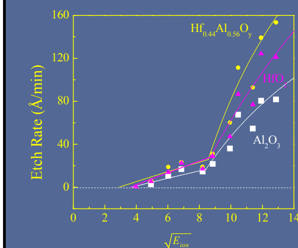

$$R_t = \frac{J_i \left[A_s \left(E_{ion}^{1/2} - E_{th,s}^{1/2}\right) + B_s \left(E_{ion}^{1/2} - E_{tr,s}^{1/2}\right)\right]}{1 + J_i \left[A_s \left(E_{ion}^{1/2} - E_{th,s}^{1/2}\right) + B_s \left(E_{ion}^{1/2} - E_{tr,s}^{1/2}\right)\right] \Big/ J_e Z_{es}}$$

$$J_i = n_s u_B = n_s \left(\frac{eT}{M}\right)^{1/2} \xrightarrow[2.63\ \text{eV}]{5.6\times10^{16}\ \text{m}^{-3}} 1.06\ \text{Cl}^+/\text{Å}^2\text{s}$$

$$J_e = \frac{P}{4RT}\left(\frac{8kT}{\pi m}\right)^{1/2} \longrightarrow 53.9\ \text{Cl/Å}^2\text{s}$$

Parameter	Range
J_i	0.6 – 0.8
J_e	45 - 60
A_s	0.1 – 0.9
B_s	0.9 – 3.9
Z_{es}	0.05 - 1
$E_{th,s}$	6 - 20
$E_{tr,s}$	8.2 – 9

Root-sum-squared (RSS) error is calculated for each $R_t = f\left(\sqrt{E_{ion}}\right)$ compared to the experimental result to obtain the best fitted curve from the combination of varying parameters

- Adequate fitting is achieved with physically reasonable values of model parameters

Modeling of ER in BCl_3

BCl_3 3 mTorr, 500 W

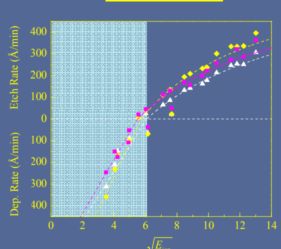

$$R_t = \frac{J_e^2 Z_{es} Z_{ep} - J_d^2 Z_{ds} Z_{dp}}{\left\{ \begin{array}{l} J_e Z_{ep} + \dfrac{J_d^2 Z_{ds} Z_{dp}}{D_p} + \dfrac{J_d J_e Z_{ds} Z_{ep}}{J_i C_p \left(E_{ion}^{1/2} - E_{th,p}^{1/2}\right)} + \\ + J_d Z_{ds} + \dfrac{J_d J_e Z_{ds} Z_{ep}}{D_s} + \dfrac{J_e^2 Z_{es} Z_{ep}}{J_i B_s \left(E_{ion}^{1/2} - E_{tr,s}^{1/2}\right)} \end{array} \right\}}$$

$$R_t = J_i C_p \left(E_{ion}^{1/2} - E_{th,p}^{1/2}\right) - J_d Z_{dp}$$

$$J_i = n_s u_B = n_s \left(\frac{eT}{M}\right)^{1/2} \xrightarrow[1.96\ \text{eV}]{4.5\times10^{16}\ \text{m}^{-3}} 0.69\ \text{BCl}_2^+/\text{Å}^2\text{s}$$

$$J_e = \frac{P}{4RT}\left(\frac{8kT}{\pi m}\right)^{1/2} \longrightarrow 52\ \text{(Cl+BCl)/Å}^2\text{s}$$

Parameter	Value
J_i	0.6 – 0.9
J_e	40 - 60
J_d	5 - 25
B_s	1 - 4
C_p	0.5 - 2
D_s	0.1 – 1.5
D_p	0.1 – 1.5

Parameter	Value
Z_{es}	0. 1 - 2
Z_{ds}	0.01 - 1
Z_{ep}	0. 1 – 1.5
Z_{dp}	0.01 - 1
$E_{tr,s}$	5 - 6
$E_{th,p}$	1.5 – 2.5

- Adequate fitting is achieved with physically reasonable values of model parameters

Plasma Etch Modeling

$$R_t = \frac{J_e^2 v_{es} S_{es} v_{ep} S_{ep} - J_d^2 v_{ds} S_{ds} v_{dp} S_{dp}}{J_e v_{ep} S_{ep} + \dfrac{J_d^2 v_{ds} S_{ds} v_{dp} S_{dp}}{D_p} + \dfrac{J_d J_e v_{ds} S_{ds} v_{ep} S_{ep}}{J_i C_p \left(E_{ion}^{1/2} - E_{th,p}^{1/2}\right)} + J_d v_{ds} S_{ds} + \dfrac{J_d J_e v_{ds} S_{ds} v_{ep} S_{ep}}{D_s} + \dfrac{J_e^2 v_{es} S_{es} v_{ep} S_{ep}}{J_i \left[A_s \left(E_{ion}^{1/2} - E_{th,s}^{1/2}\right) + B_s \left(E_{ion}^{1/2} - E_{tr,s}^{1/2}\right)\right]}}$$

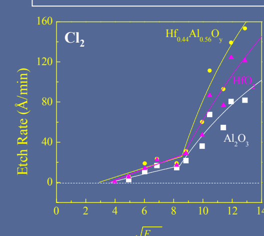

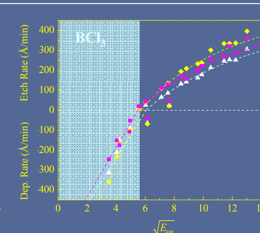

- The model address flux/energy dependence and etch/deposition competition

Nanoscale Patterning of Oxides

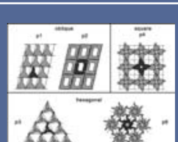

U. B. Sleytr et al. Progress in Surf. Sci. 68, 231 (2001).

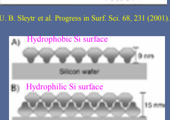

* E. S. Gyorvary et al. J. Microscopy 212, 300 (2003).

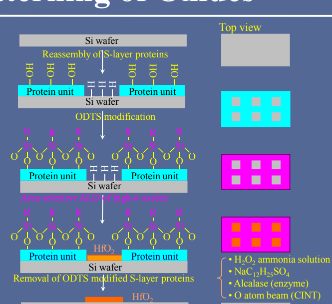

- Area-selective ALD for nano-scale patterning of multifunctional oxides

Liu, Chang et. al. JACS (2008)

Conclusions

- Multifunctional metal oxides have numerous applications
- Well controlled doping in metal oxides can be accomplished by atomic layer deposition
- Effective patterning of metal oxides by chlorine based plasmas
  - Etch rate scales with the square root of E_{ion}
  - Etching product distributions depends strongly on ion energy
- A comprehensive reaction model accounts for etch/deposition
  - Captures basic etch rate dependencies on fluxes and ion energy
  - Highlights the importance of competitive mechanisms
- Plasma patterning enables the integration of multifunctional materials